Biocompatibility and osteogenesis of the castor bean polymer doped with silica (SiO_2) or barium titanate ($BaTiO_3$) nanoparticles[1]

Renato Silva Nacer[I], Baldomero Antonio Kato da Silva[II], Rodrigo Ré Poppi[III], Dheywid Karlos Mattos Silva[IV], Vinicius Saura Cardoso[V], José Renato Jurkevicz Delben[VI], Angela Antonia Sanches Tardivo Delben[VII]

DOI: http://dx.doi.org/10.1590/S0102-865020150040000004

[I]Fellow PhD degree, Postgraduate Program in Health and Development, West Central Region, Federal University of Mato Grosso do Sul (UFMS), Campo Grande-MS, Brazil. Design, intellectual and scientific content of the study.
[II]PhD, Associate Professor, Postgraduate Program in Biomedical Science, Federal University of Piaui (UFPI), Parnaiba-PI, Brazil. Acquisition of data, statistical analysis, critical revision.
[III]Fellow PhD degree, Postgraduate Program in Health and Development, West Central Region, UFMS, Campo Grande-MS, Brazil. Technical procedures, manuscript preparation.
[IV]Master, Associate Professor, Veterinary Department, University Center of Grande Dourados (UNIGRAN), Dourados-MS, Brazil. Technical procedures, histopathologic examinations.
[V]PhD, Associate Professor, Physical Therapy Department, UFPI, Parnaiba-PI, Brazil. Histomorphometric examinations, interpretation of data.
[VI]PhD, Associate Professor, Physics Department, UFMS, Campo Grande-MS, Brazil. Synthesis and production of biomaterials.
[VII]PhD, Associate Professor, Physics Department, UFMS, Campo Grande-MS, Brazil. Conception of the study, critical revision.

ABSTRACT

PURPOSE: To evaluate the biocompatibility and osteogenesis of castor oil polymer doped with SiO_2 or $BaTiO_3$ nanoparticles.

METHODS: Twenty four male rats Wistar were submitted to bone defect filled with castor oil polymer. The animals were distributed in two experimental groups had been formed with 12 animals each: Group 1 - Castor oil polymer doped with 0.30 grams of SiO_2 replacing 0.30 grams of $CaCO_3$. Group 2 - Castor oil polymer doped with 0.30 grams of $BaTiO_3$ replacing 0.30 grams of $CaCO_3$. Euthanasia occurred 30 and 60 days after surgery and the femurs were sent to histological analysis and MEV.

RESULTS: The implants were biocompatible and allowed for progressive osteogenesis through osteoconduction in both observation periods. There was significant bone neoformation at 30 and 60 days in both groups within the histomorphometric evaluation, but group 1's osteogenesis was lesser in the 30 and 60-day periods observed when compared to the animals of group 2. The MEV morphometric evaluation evidenced a lesser percentage of osseous tissue filling within the BaTiO2-doped polymer.

CONCLUSION: The castor oil polymer doped with SiO2 or BaTiO3 remained biocompatible and allowed for progressive osteogenesis in both observation periods.

Key words: Biocompatible Materials. Osteogenesis. Castor Oil. Nanoparticles. Rats.

Introduction

The history of tissue repair using biomaterials can be traced back to the Prehistoric Period and, during a long time, happened in a very empirical manner, expecting only they would be inert, non-toxic and well-tolerated[1]. The evolution in the biomaterials' employ involved the search of devices that stimulated the implant's integration with the nearest tissues through cellular activation, proliferation and differentiation in the implant's site, as well as the subsequent formation of the extracellular matrix intimately associated with the implanted material[2].

Among all the favorable aspects expected in a biomaterial, allowing for osteogenesis in the bone-implant interface, optimizing the osteoblasts' differentiation, is primordial from a clinical point of view[3]. In this sense, porous materials that work as support for bone growth, working as an outline that ensures the cellular infiltration to the implant's interior, have become noticed and are highly applied in experimental studies[4].

Experimental studies have shown the applicability *in vivo*[5,6] and the benefits for castor oil polymer *in vitro*[7,8], revealing the biocompatibility, osteointegration and, mainly, the diameter, conformation and intercommunication of the pores as the most important aspects to regulate vascular and cellular migration to the inside of these implants, allowing for bone neoformation.

However, despite the advantages presented by the castor oil polymer, an implant will hardly harbor all the ideal properties for bone replacement, especially when compared to autogenous grafts. In this context, the development of new composite materials that resemble natural bone structure, and capable of concentrating traits so as to ease osteogenesis promotion, has been the challenge of many researchers[9].

Many studies pointed out promising results in the use of mesoporous silica (SiO_2) based biomaterials in osseous tissue repair processes[10,11]. According to Colilla *et al.*[12], when these biomaterials are exposed to physiological environment, a series of chemical reactions happen in the tissue/material interface, leading to the material's incorporation to the living tissue.

Other studies have sought new ways to stimulate osteogenesis, through electrically-charged materials[13]. Studies involving piezoelectric ceramics for implantation were focused, for the most part, in materials containing barium titanate ($BaTiO_3$). $BaTiO_3$ is a ferroelectric ceramic characterized by the presence of spontaneous polarization and the ability to guide osteogenesis towards polarization. Just like with the bone, the source of piezoelectric behavior in electric iron materials comes from the formation of an electric dipole due to an asymmetrical ion distribution[14].

The study of the interaction of bioceramics with distinct osteogenic traits in the production of composite biomaterials, aiming to optimize the implant's properties, will allow for the development of an ideal framework for bone regeneration. As such, the aim of this study was to evaluate the biocompatibility and osteogenesis of castor oil polymer doped with SiO_2 or $BaTiO_3$ nanoparticles.

Methods

All the experimental procedures were analyzed and approved by the Ethic Committee in the Use of Animals of UFMS with protocol number 494/2013 and complied with the Council for International Organization of Medical Sciences (CIOMS)'s ethical code for animal experimentation.

Implants' presentation and preparation

The implants were prepared following the instructions recommended by the maker (BIOMECÂNICA Ind. e Com. de Prod. Ortopédicos Ltda). Castor oil polymer is obtained by mixing the pre-polymer and poliol (Liquid fraction), and the calcium carbonate ($CaCO_3$) (Powder fraction) is added to the polyurethane's basic components aiming to give it porosity and improve the base resistance and elasticity[9,10].

The SiO_2 nanoparticles were prepared by the UFMS Materials group through Microemulsion mediated sol-gel and the particle size control was taken through surfactant usage. The BaTiO3 nanoparticles were prepared by the University Center of Grande Dourados (UFGD)'s Physics Department and synthesized through High-Energy Ball Milling (HEBM). Both nanostructured particles had a clear, dry powder state.

To prepare the biomaterial blocks, the components were inserted into a Becker and weighed individually, in preset proportions per group, and with each component insertion, the weighs were zeroed for the next insertion. After all components were inserted, they were mixed until they gained an aspect of mass with great adherence.

Afterwards, the biomaterial was placed in a Teflon plate and pressed to create blocks 1.00mm thick with a diameter 2.00mm wide. The blocks obtained were sterilized individually through ethylene oxide to be used in the operatory procedure.

Animal characteristics and formation of experimental groups

Twenty-four Wistar rats, adult males, weighing between 250 and 300 grams, aged three months, were obtained from UNIGRAN's Central Animal Laboratory. Throughout the entire

experiment the animals were kept in 12 hour photoperiods, with minimal noise, solid rations and water *ad libitum*, staying under watch for a period of two days, before their use in the experiment.

The animals were spread randomly in two distinct experimental groups, according to the implanted material. In group 1's animals, the bone defect was filled with castor oil polymer doped with 0.30 grams of SiO_2, equal to 10% the powder fraction, replacing 0.30 grams of $CaCO_3$. In group 2, the animals had their bone defect filled with castor oil polymer implants with 0.30 grams of $BaTiO_3$ (10% of the Powder fraction) added, replacing 0,30 grams of $CaCO_3$.

Surgical procedure

After a semiologic exam realized by the veterinarian, the animals received pre-anesthetic medication with Ketamine at 5% (50mg/kg) (Sepso Ind. e Com. Ltda, Jacareí, SP) plus Xilasina a 2% (10mg/kg) (Sepso Ind. e Com. Ltda, Jacareí, SP), through intra-peritoneal and for anesthetic maintenance Isoflurane was administered via inhalation, through a facial cone with oxygen and universal vaporizer with a 1 $L.min^{-1}$ flux.

Having stated the anesthetic plan, the animals were placed for fur rasping on the side of their lower right leg. With aseptic technique, access to the diaphysis of the femur in the proximal (cranium-lateral) side was performed for confection of the bone defect. After bone exposure, a defect of 2mm diameter was performed using a spheric-type #1016 (KG Sorensen) diamond-tipped drill under constant irrigation with physiological serum perforating the bone cortical until reaching the medullar canal. After implanting the composite, synthesis through plans with polyamide nylon 0.30 needlepoint was performed.

Immediately after surgery and through four consecutive days (24/24 hours), the animals received anti-inflammatory and analgesic flunixin meglumine (Banamine® - Schering-Plough, Indústria Brasileira) medication administered intraperitoneally at doses of 1.1 mg/kg.

Euthanasia

After the 30 and 60-day observation periods, the animals were submitted to euthanasia with intraperitoneal infusion of lethal dose of sodium Thiopental (120mg/ml).

Histomorphometric and morphometric through Scanning Electron Microscopy (SEM)

The total areas of the implant and bone neoformation, both in the histological blade images, as in the images taken through SEM, were calculated through the manual delimitation of areas and the measuring was made using the ImageJ 1.0 for Mac program. Initial measurements for the areas (pixels) were converted to μm, at a 1 to 6.25 proportion (1 pixel = 6.25 μm). For statistical analysis the proportions of bone neoformation were considered, through the quotient between the neoformation area and the total defect area (proportion of neoformed bone: neoformed bone area/ total defect area), being expressed as a percentage.

Images of the blades destined to histomorphometric scans were captured through an Olympus® Japan - BX41 light microscope, tinted with Hematoxylin and Eosin and the standardized 10X increase to allow for general observation of the implanted area and the nearby tissue.

To obtain the SEM images a JEOL-brand JSM-6380LV-model scanning electron microscope from UFMS' Multiuser Laboratory of Materials Analysis (MULTILAM) was used. The images of the transversally-sectioned pieces, sent for morphometric analysis in the SEM, were captured using Backscattering Electrons (BSE), which allow for a contrast increase between structures of different compositions and densities, favoring the differentiation between the implant and osseous tissue.

Statistical analysis

Data was organized so as to compare the percentage values of bone neoformation in relation to the implanted polymer area. Intergroup comparisons were performed through the Mann-Whitney Test. The significance level considered was 95% ($p<0.05$). Biocompatibility, traits in the process of tissue neoformation, osteogenesis and the morphological and structural aspects of the biomaterials were analyzed and the results are expressed in a descriptive manner.

Results

All animals had an uneventful postoperative course and exhibited normal behavior. The presence of SiO_2 or $BaTiO_3$ in the castor oil polymer did not affect the material's properties, which remained biocompatible, retained the internal porosity, and revealed itself to be capable of promoting osteoconduction.

Descriptive histopathological evaluation

In Group 1's animals, after 30 days, small areas of bone neoformation in the bone-implant interface were noticed.

Aside from the apposition of neoformed osseous tissue in the edges of the bone defect, discreet osteogenic activity towards the implanted material's interior was noticed. After 60 days, increase of bone growth around and inside the implant was observed, with abundant presence of mature osseous tissue and intense fibroblastic activity producing the collagenous matrix that precedes bone mineralization. The bone occupation within the biomaterial reinforces the osteointegration trait and suggests that the castor oil polymer doped with SiO_2 can be reabsorbed (Figure 1).

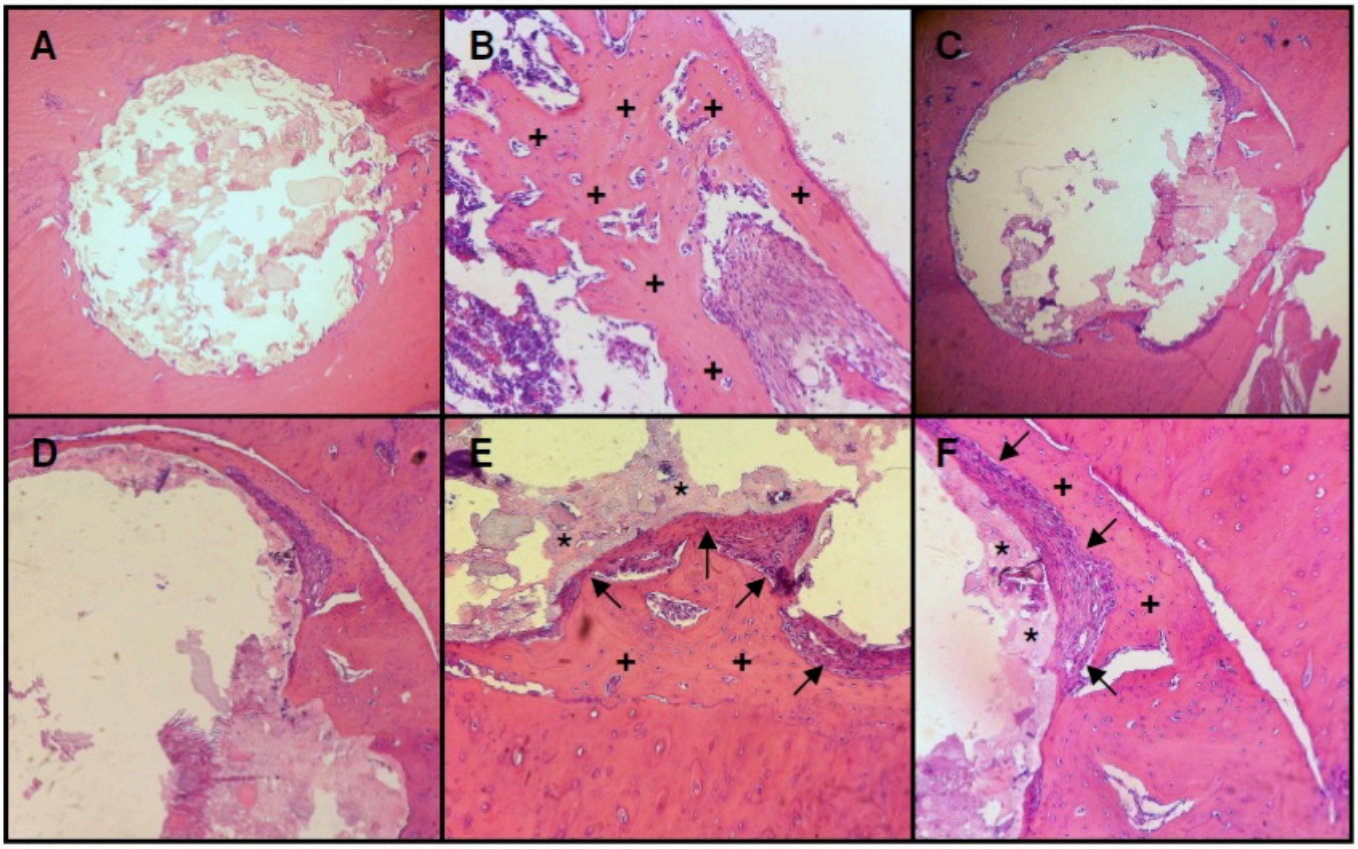

FIGURE 1 – G1 photomicrograph montage: **A** and **B** (30 Days) – General view of implant site. Mature bone tissue (+) occupying material's border. **A**-HE, x10; **B**-HE, x40. **C, D, E, F** (60 Days) – Fibroblastic activity (↑) which precedes osteogenesis between biomaterial (*) and neoformed mature bone tissue (+). **C**-HE, x10; **D**-HE, x20; **E** and **F**-HE, x40.

G2's animals' histological evaluation at 30 days revealed discreet bone neoformation around the implant, however, with intense fibroblastic activity towards the defect's interior, characterizing the formation of the immature bone matrix that will replace the mature osseous tissue. As well, the presence of osteoclasts promoting material degradation for posterior osteogenesis is noticed. At 60 days, the bone defect was partially occupied by lamellar bone rich in osteocytes, few inflammatory mononuclear cells, and reduction in osteoblastic activity. Great proximity of mature osseous tissue with the biomaterial was noticed as well, suggesting osteointegration (Figure 2).

Scanning electron microscopy: descriptive morphological evaluation

Images obtained through secondary electrons (SE) and through backscattering electrons (BSE) of the animals belonging to group 1, with 30 days of observation, displayed endosteum bone growth, well-integrated interface between the neoformed bone and the implant and the biomaterial's pores displaying abundant osteoprogenitor cell activity secreting the initial bone matrix. After 60 days of observation, the implants matching group 1's animals were wrapped by osseous tissue. The bone neoformation happened through the periosteum and endosteum, small pores next to the interface were filled by mature osseous tissue and the implant remains integrated to the bone through an immature, still forming bone matrix (Figure 3).

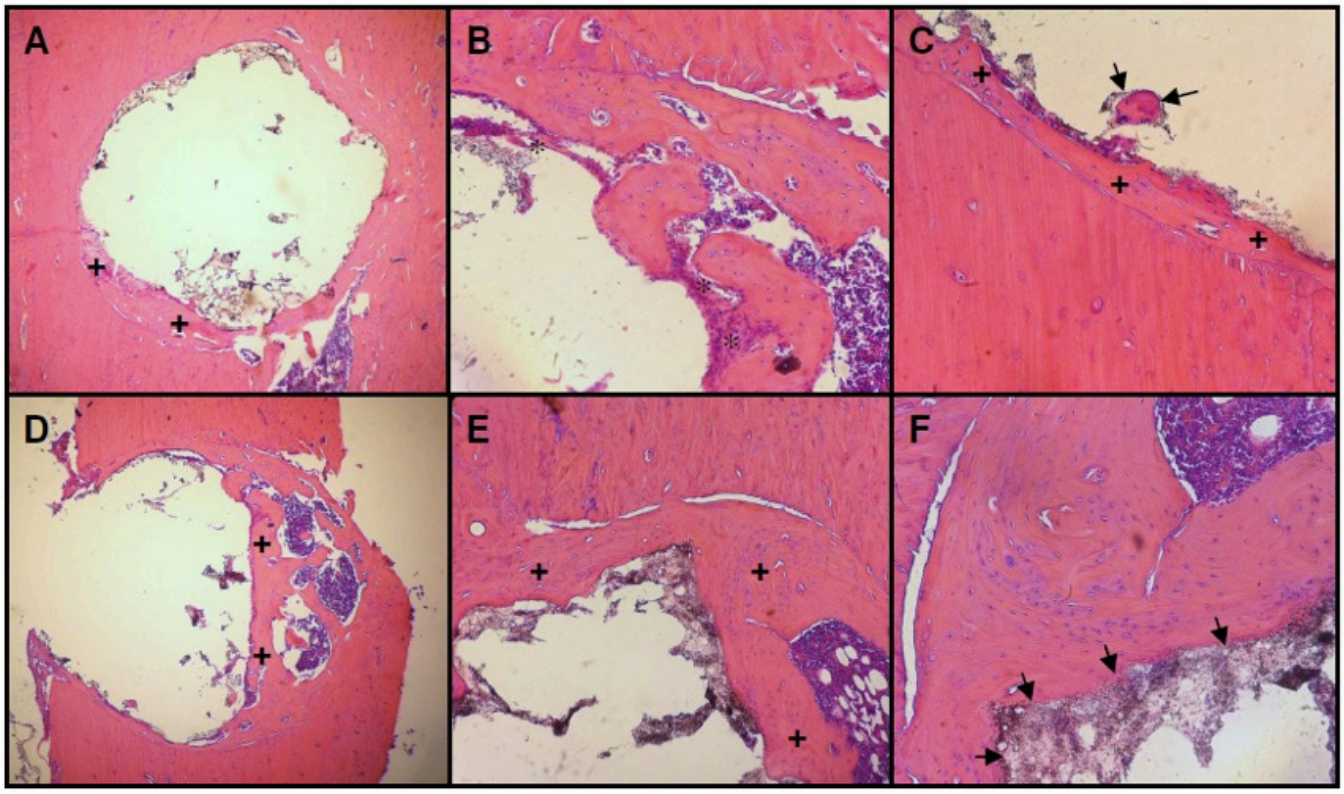

FIGURE 2 – G2's blades' photomicrograph montage: **A**, **B** and **C** (30 days) – Neoformed bone in the interface (+), with fibroblastic activity forming osteoid matrix (*) and osteoclast absorbing material (↑). **A**-HE, x10; **B**-HE, x40; **C**-HE, x100. **D, E, F** (60 Days) – Mature bone inside biomaterial (+) and integration between polymer and bone (↑). **D**-HE, x10; **E**-HE, x20; **F**-HE, x100.

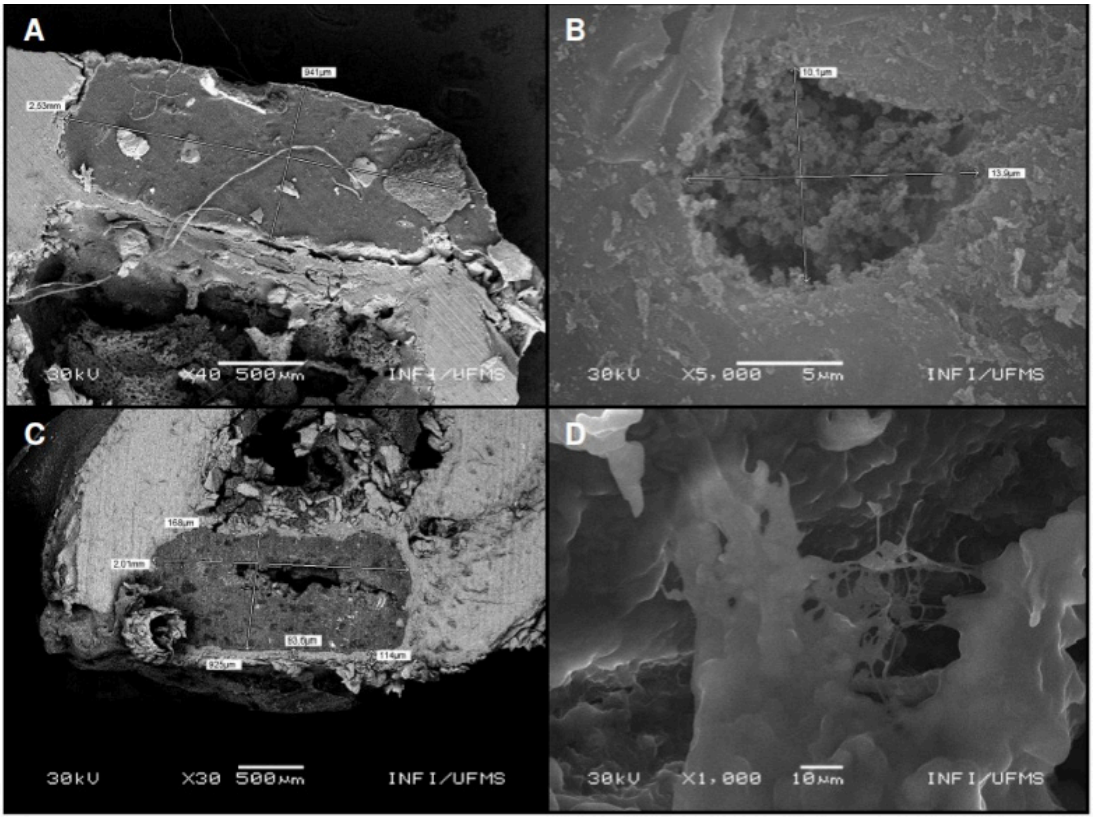

FIGURE 3 – Group 1's animals' MEV-taken photomicrograph montage after 30 (**A** and **B**) and 60 (**C** and **D**) days of observation. **A** – Implant's transversal dimensions. BSE, x40. **B** – Biomaterial's pores containing osteoprogenitor cells in activity. SE, x5000. **C –** General view of implant and the transversal dimensions of the biomaterial and neoformed bone tissue. BSE, x30. **D** – Immature bone matrix being formed in the bone-implant interface. SE, x1000.

Group 2's animals, after 30 days of implanting, displayed discreet osteogenesis and little cell activity around the implant. The material remained well coapted with the neoformed bone around it, even with alterations of the biomaterial's surface in relation to the bone. At 60 days, there was increase of osteogenesis in the interface, with bone growth towards the inside of the biomaterial, however, there was little bone neoformation happening through the periosteum and endosteum. A few pores of varying diameters were noticed next to the interface, filled in with mature osseous tissue, and osteogenic cells promoting bone formation over the implant (Figure 4).

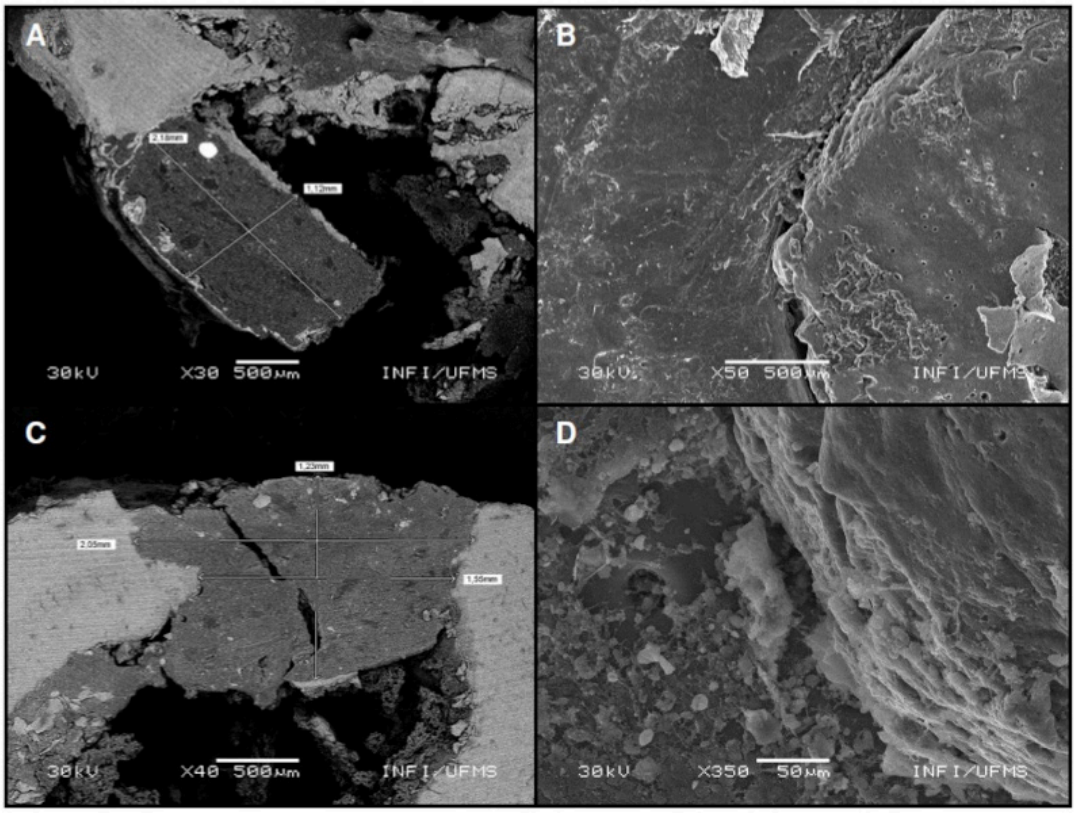

FIGURE 4 – Group 2's animals' MEV-taken photomicrograph montage after 30 (**A** and **B**) and 60 (**C** and **D**) days of observation. **A** – General view and transversal dimensions of biomaterial. BSE, x30. **B** – Implant-bone interface topograph. SE, x50. **C** – Transversal dimensions of biomaterial and bone-implant interface. BSE, x40. **D** – Osteogenic cells promoting bone formation. SE, x350.

Histomorphometric analysis

The results of the histomorphometric analysis of the groups and periods studied are represented on Tables 1 and 2, and Figures 5 to 8.

TABLE 1 - Intergroup comparison of average values ± standard deviation of bone neoformation percentage in relation to implanted polymer area.

	Group 1	Group 2	p-value
MEV			
30 days	20.2±0.6	16.7±3.1	0.0209
60 days	29.0±13.8	25.1±2.2	0.2482
Histological Analysis			
30 days	19.6±1.7	22.3±2.6	0.0433
60 days	28.0±7.6	32.8±1.8	0.3367

TABLE 2 - Intragroup comparison of average values ± standard deviation of bone neoformation percentage in relation to implanted polymer area.

GROUP	30 days	60 days	p-value
MEV			
Group 1	20.2±.,6	29.0±13.8	0.3760
Group 2	16.7±3.1	25.1±2.2	0.0048
Histological Analysis			
Group 1	19.6±1.7	28.0±7.6	0.0298
Group 2	22.3±2.6	32.8±1.8	0.0039

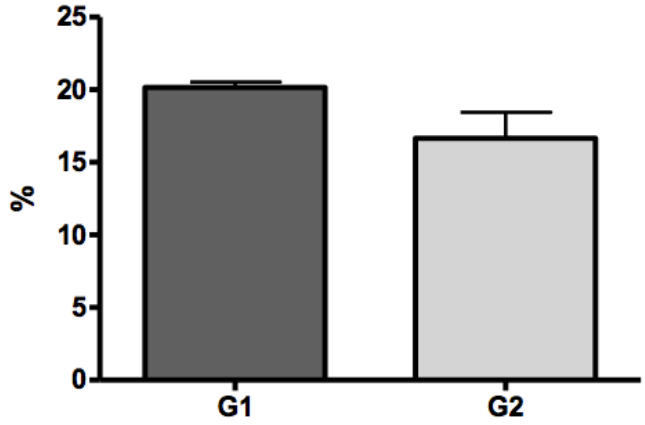

FIGURE 5 - Comparison of the value averages of bone neoformation in relation to implanted polymer area to the MEV reading after 30-day experiment period (Mann-Whitney, p = 0.0209).

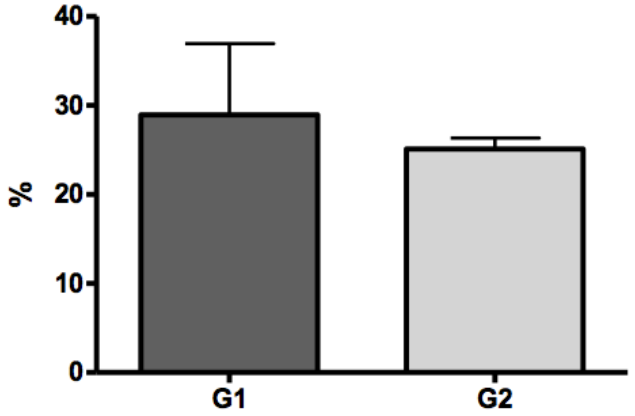

FIGURE 6 - Comparison of the value averages of bone neoformation in relation to implanted polymer area to the MEV reading after 60-day experiment period (Mann-Whitney, p = 0.2482).

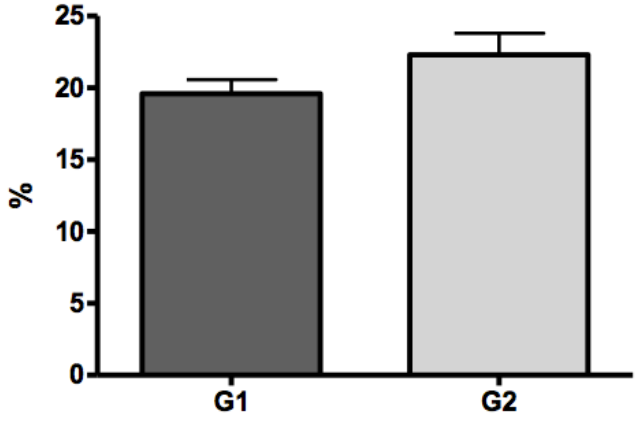

FIGURE 7 - Comparison of the value averages of bone neoformation in relation to implanted polymer area to the histological analysis after 30-day experiment period (Mann-Whitney, p = 0.0433).

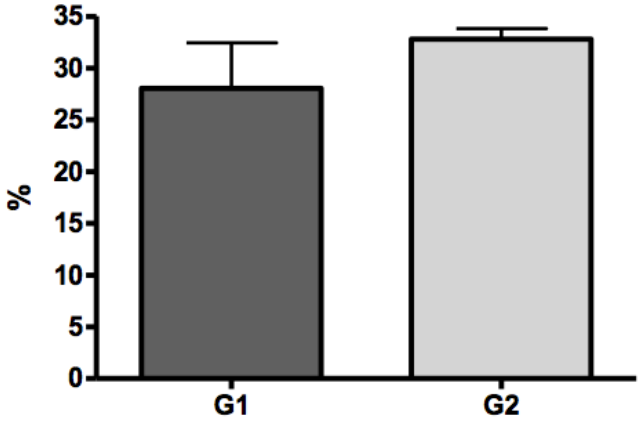

FIGURE 8 - Comparison of the value averages of bone neoformation in relation to implanted polymer area to the histological analysis after 60-day experiment period (Mann-Whitney, p = 0.3367).

Discussion

Many studies[5,7,10] point out the advantages of using castor oil polymer as a framework for bone growth, however, castor oil polymer integrates itself to the receiving bone in a slower and more incomplete manner when compared to autogenous bone graft[15], especially for not displaying specific biological traits.

In the present study, the animals of group 1 received castor oil polymer implants doped with SiO_2 and the animals of group 2 with $BaTiO_3$, both replacing the equivalent to 10% of $CaCO_3$ in their respective groups, with the aim of optimizing the material's characteristics. Morphometric intragroup analysis of the bone neoformation percentage in relation to the polymer implant area showed there was significant increase of osteogenesis around and within the polymer in both groups.

Saran *et al*.[9] also stated the osteogenesis progression after implanting castor oil polymer in the medullar canal of rabbit tibia. According to the authors, at the 90-day post-implant period, deposition of immature osseous tissue in contact with the implant could still be observed. The neoformed bone around the biomaterial took on a lamellar aspect as time went on, after 120 and 150 days of observation.

Del Carlo *et al*.[16] observed the migration of osteoprogenitor cells invading the surface porous structure of castor oil polymer, followed by the direct bone deposition and concluded that castor oil polymer behaves like a passive framework that allows for progressive bone neoformation and osteoconduction, however, the biomaterial was not capable of promoting osteoinduction.

According to Leonel *et al*.[17], castor oil polymer revealed itself to be a supporting material to the regenerative process of bone defects created experimentally in the zygomatic arc of rats.

To the authors, bone neoformation, which was greater in the final periods of examination, happened through osteoconduction, given that castor oil polymer allowed for tissue growth among its pores and over its external surface since the starting periods of observation.

In this study, at the end of the observation period (60 days), there was no meaningful difference with regards to the percentage of bone neoformation around and within the implants during intergroup comparison, which suggests similarity in the nanoparticles' osteogenetic potential.

The biological behavior of the SiO_2 and $BaTiO_3$ nanoparticles, as well as the manner which each ceramic stimulates osteogenesis, is quite divergent. While SiO_2 has an important role in living tissue biomineralization and its ability to induce osteoprogenitory cells to the lesion's location[18], BaTiO3 stimulates bone neoformation due to its dielectric and piezoelectric properties[14].

Nacer *et al.*[10] evaluated the castor oil polymer doped with silica nanoparticles' *in vivo* behavior, and confirmed an increase in number of osteoprogenitory cells around and within the composite when compared to the isolated castor oil polymer implant. According to the authors, the success of castor oil polymer with 10% silica can be attributed to SiO_2's osteoinducing nature, along with the nanoparticles altering the support's morphology, granting great coarseness to the external surface.

According to Henson and Getgood[19], the presence of silica nanoparticles added in scaffolds has an important role in osteogenesis, for they can simulate the extracellular matrix's internal architecture, fundamental tissue-material interaction.

Terriza *et al*.[20], upon evaluating SiO_2's biocompatibility and bioactivity in poly (D,L-lactic acid lactic-co-glycolic acid) (PLGA), concluded that bioactive inorganic materials, like SiO_2 granulates, improve synthetic biopolymers' osteogenic performance due to their excellent chemical stability and the tight relationship between silicate and calcium deposition on its surface.

Studies centered in utilizing electrically-charged materials have shown promising results in stimulating osteogenesis. Feng *et al*.[21] implanted hydroxyapatite and $BaTiO_3$ ceramics in dog mandibles and confirmed that $BaTiO_3$ implants promoted greater growth and bone repair. According to the authors, tissue growth around the implant happened in an orderly manner, which increased the efficacy of osteogenesis in the $BaTiO_3$ ceramic's surface. Yu *et al*.[22] concluded that BaTiO3's piezoelectric capacity is greater when implanted, when compared to synthetic hydroxyapatite.

Ciofani *et al*.[23] evaluated the effects of barium titanate nanoparticles over proliferation and differentiation of the mesenquimal cells of rats, and concluded that the $BaTiO_3$ nanoparticles promoted a meaningful increase in the formation of hydroxyapatite deposits during bone neoformation.

Conclusion

Castor oil polymer doped with $BaTiO_3$ or SiO_2 nanoparticles behaved like a biocompatible framework, capable of allowing for progressive bone neoformation within its communicative porous structure, promoting induction and aggregation of bone cells over its surface and, subsequently, speed up the osteogenesis process.

References

1. Wu S, Liu X, Yeung KW, Liu C, Yang X. Biomimetic porous scaffolds for bone tissue engineering. Mat Sci Eng. 2014 Jun;80(1):1-36. doi: 10.1016/j.mser.2014.04.001.
2. Mavrogenis AF, Dimitriou R, Parvizi J, Babis GJ. Biology of implant osseointegration. J Musculoskelet Neuronal Interact. 2009 Apr-Jun;9(2):61-71. PMID: 19516081.
3. Singhatanadgit W. Biological responses to new advanced surface modifications of endosseous medical implants. Bone Tissue Regeneration Insights. 2009;2:1-11.
4. Hertz A, Bruce IJ. Inorganic materials for bone repair or replacement applications Nanomedicine (Lond). 2007 Dec;2(6):899-918. doi 10.2217/17435889.2.6.899.
5. Pereira-Júnior OC, Rahal SC, Iamaguti P, Felisbino SL, Pavan PT, Vulcano LC. Comparison between polyurethanes containing castor oil (soft segment) and cancellous bone autograft in the treatment of segmental bone defect induced in rabbits. J Biomater Appl. 2007 Jan;21(3):283-97. doi: 10.1177/0885328206063526.
6. Belmonte GC, Catanzaro-Guimarães SA, Sousa TPT, Carvalho RS, Kinoshita A. Qualitative histologic evaluation of the tissue reaction to the polyurethane resin (*Ricinus communis* – based biopolymer) implantation assessed by light and scanning electron microscopy. Polímeros. 2013 Jan;23(4):462-7. doi: http://dx.doi.org/10. 4322/polimeros.2013.063.
7. Barros VM, Rosa AL, Beloti MM, Chierice G. *In vivo* biocompatibility of three different chemical compositions of *Riccinus communis* polyurethane. J Biomed Mater Res A. 2003 Oct 1;67(1):235-9. PMID: 14517881.
8. Pereira-Júnior OC, Rahal SC, Lima-Neto JF, Landim-Alvarenga FC, Monteiro FOB. In vitro evaluation of three different biomaterials as scaffolds for canine mesenchymal stem cells. Acta Cir Bras. 2013 May;28 (5):353-60. http://dx.doi.org/10.1590/S0102-86502013000500006.
9. Saran WR, Chierice GO, Silva RAB, Queiroz AM, Silva FWGP, Silva LAB. Castor oil polymer induces bone formation with high matrix metalloproteinase-2 expression. J Biomed Mater Res A. 2014 Feb;102(2):324-31. doi: 10.1002/jbm.a.34696.
10. Nacer RS, Poppi RR, Carvalho PTC, Silva BAK, Odashiro AN, Silva IS, Delben JRJ, Delben AAST. Castor oil polyurethane containing silica nanoparticles as filling material of bone defect in rats. Acta Cir Bras. 2012 Jan;27(1):56-62. http://dx.doi.org/ 10.1590/S0102-86502012000100010.
11. Arcos D, Izquierdo-Barba I, Vallet-Regı M. Promising trends of bioceramics in the biomaterials Field. J Mater Sci Mater Med. 2009

Feb;20:447–55. doi: 10.1007/s10856-008-3616-x.
12. Colilla M, Manzano M, Vallet-Regí M. Recent advances in ceramic implants as drug delivery systems for biomedical applications. Int J Nanomedicine. 2008 Dec;3(4):403–14. PMID: 19337409.
13. Furuya K, Morita Y, Tanaka K, Katayama T, Nakamachi E. Acceleration of osteogenesis by using barium titanate piezoelectric ceramic as an implant material. Bioinspiration, Biomimetics, and Bioreplication. 2011 May; 7975. http://dx.doi.org/10.1117/12.881858.
14. Baxter FR, Bowen CR, Turner IG, Dent ACE. Electrically active bioceramics: a review of interfacial responses. Ann Biomed Eng. 2010 Jun;38(6):2079-92. doi: 10.1007/s10439-010-9977-6
15. Jacques JW, Fagundes DJ, Figueiredo AS, Inouye CM, Scapulatempo RP, Sassioto MCP. O papel da poliuretana de mamona como substituto do enxerto ósseo autógeno em coelhos. Rev Col Bras Cir. 2004 Jul;31(4):236-41. http://dx.doi.org/10.15 90/S0100-69912004000400005.
16. Del Carlo RJ, Kawata D, Viloria MIV, Oliveira DR, Silva AS, Marchesi DR, Galvão SR, Azevedo P, Monteiro BS. Polímero derivado de mamona acrescido de cálcio, associado ou não à medula óssea autógena na reparação de falhas ósseas. Cienc Rural. 2003 Dec;33(6):1081-8. http://dx.doi.org/10.1590/S0103-84782003000600013.
17. Leonel ECF, Andrade Sobrinho J, Oliveira Ramalho LT, Porciúna HF, Mangilli R. A ação do polímero de mamona durante a neoformação óssea. Acta Cir. Bras. 2004 Aug;19(4):342-50. http://dx.doi.org/10.1590/S0102-86502004000400005.
18. Andrade AL, Domingues RZ. Cerâmicas bioativas – Estado da arte. Quím Nova 2006 Feb;29(1):100-4. http://dx.doi.org/10.1590/S0100-40422006000100019.
19. Henson F, Getgood A. The use of scaffolds in musculoskeletal tissue engineering. Open Orthop J. 2011 Jul;5(2):261-6. doi: 10.2174/1874325001105010261.
20. Terriza A, Vilches-Pérez JI, Orden E, Yubero F, Gonzalez-Caballero JL, González-Elipe AR, Vilches J, Salido M. Osteoconductive potential of barrier NanoSiO2 PLGA membranes functionalized by plasma enhanced chemical vapour deposition. Biomed Res Int. 2014 May;2014:253590. doi: 10.1155/2014/253590.
21. Feng JQ, Yuan HP, Zhang XD. Promotion of osteogenesis by a piezoelectric biological ceramic. Biomaterials. 1997 Dec;18:1531–4. doi: 10.1016/S0142-9612(97)80004-X.
22. Yu SW, Kuo ST, Tuan WH, Tsai YY, Wang SF. Cytotoxicity and degradation behavior of potassium sodium niobate piezoelectric ceramics. Ceramics Int. 2012 May;38(4):2845–50. doi: 10.1016/j.ceramint.2011.11.056.
23. Ciofani G, Ricotti L, Canalec C, D'Alessandro D, Berrettini S, Mazzolaia B, Mattolia V. Effects of barium titanate nanoparticles on proliferation and differentiation of rat mesenchymal stem cells. Colloids Surf B Biointerfaces. 2013 Feb 1;102:312-20. doi: 10.1016/j.colsurfb.2012.08.001.

Acknowledgement

To Biomecânica Ind. e Com. de Prod. Ortopédicos Ltda for providing the castor bean polymer.

Correspondence:
Renato Silva Nacer
Travessa João Domingos, 231/casa 04
79050-032 Campo Grande – MS Brasil
Tel.: (55 67)9207-5182
renatosnacer@gmail.com

Received: Dec 19, 2014
Review: Feb 20, 2015
Accepted: Mar 18, 2015
Conflict of interest: none
Financial source: none

[1]Research performed at Veterinary Hospital, University Center of Grande Dourados (UNIGRAN), Dourados-MS, and Physics Department, Federal University of Mato Grosso do Sul (UFMS), Brazil. Part of PhD degree thesis, Postgraduate Program in Health and Development, UFMS. Tutor: Angela Antonia Sanches Tardivo Delben.